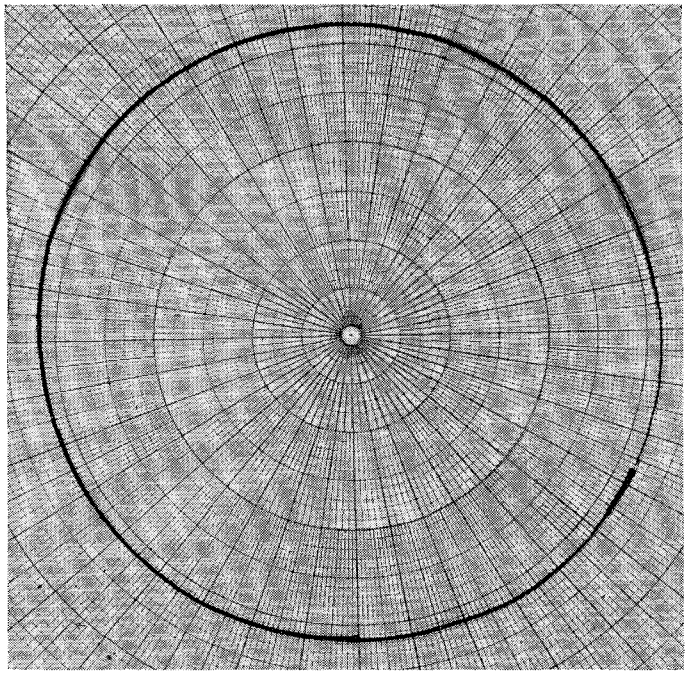

Fig. 11—Position of shorts set for circular polarization with rectangular horn removed and circular horn placed on turnstile $f=9{,}070$ mcs.

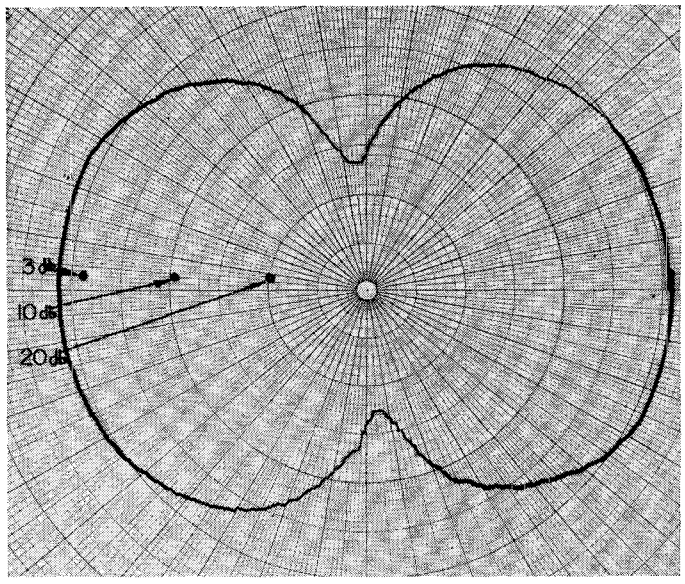

Fig. 12—Linear case, max. radar signal $f=9{,}070$ mcs.

was no canceller, and elevation where the canceller had been set to give a 68 db cancellation. The difference between a static measurement and a dynamic measurement can be accounted for by the fact that the circularity of the secondary beam breaks up at off angles due to the diffraction of the primary beam at the edges of the reflector surface.

Figs. 10–12 are recordings of the primary pattern polarization as determined from the turnstile short positions for optimum corner reflector cancellation.

Fig. 10 is the circular polarization with the pyramidal horn terminating the turnstile. In order to show the effects of this horn it was replaced with a circular horn keeping the same positions for the shorts in the turnstile arms. The pattern becomes elliptical to the extent of about 1.5 db. The final figure is a plot of the linear polarization with the pyramidal horn replaced on the turnstile. These values were recorded at 9,070 mcs.

The polarizer looks quite successful, but it bears more investigation. In the near future more quantitative data will be available for a better evaluation over existing polarizing systems.

Graphical Filter Analysis*

HARVEL N. DAWIRS†

Summary—**Some well known principles of filters and transmission lines are recalled and used to develop graphical methods of analyzing lossless transmission line filters consisting of a series of symmetrical and identical sections. The results of this development are used to construct a special filter analysis chart by means of which a filter may be completely analyzed from a Smith Chart plot of the input impedance characteristics.**

Introduction

FILTER calculations may become quite difficult in the microwave region where filter circuits are constructed of transmission line sections, since the equations involved are usually transcendental. However the important properties of lossless filters consisting of a series of symmetrical sections may be determined graphically on a Smith chart[1,2] by methods described in this paper. These methods may also be useful in analyzing mechanical filters in which the elements are essentially mechanical transmission lines.

It is to be noted that, while the methods presented are particularly adapted to transmission line circuits,

* This work was supported by a contract between Wright Air Development Center, and the Ohio State University Research Foundation.

† Department of Electrical Engineering, Ohio State University Research Foundation, Columbus, Ohio.

[1] P. H. Smith, "A transmission line calculator," *Electronics*, vol. 12, pp. 29–31; January, 1939.

[2] P. H. Smith, "An improved transmission line calculator," *Electronics*, vol. 17, pp. 130–132, 318–325; January, 1944.

they are valid for any lossless filter consisting of symmetrical sections.

Let a series of identical and symmetrical filter sections having a characteristic impedance of z_c and a propagation constant of $\gamma_1=\alpha_1+j\beta_1$ per section, be terminated in an impedance of z_L as shown in Fig. 1.

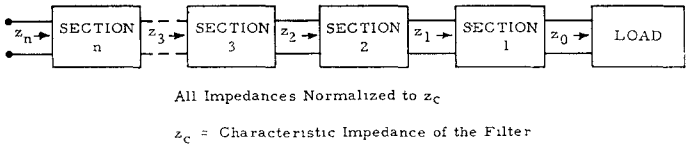

Fig. 1—Typical n-section filter.

Let $z_n=r_n+jx_n$ be the impedance normalized to z_c, and

$$k_n = \frac{z_n - 1}{z_n + 1}$$

be the voltage reflection coefficient with respect to z_c, looking into the n^{th} section as shown in Fig. 1. (Note that $z_0=z_L/z_c$.)

It is well known that the propagation constant of n sections is

$$\gamma_n = n\gamma_1, \tag{1}$$

and that

$$k_n = k_0 \exp(-2\gamma_n) = k_0 \exp(-2n\gamma_1). \tag{2}$$

In general the characteristic impedance z_c is complex, as in the familiar case of a lossy transmission line, and the normalized input impedances, z_n, $n=1, 2, \cdots$, lie on a logarthmic spiral about the center of the chart as shown in Fig. 2, on the facing page. The angle between any two points is 2β and $|k_n| = |k_0| \exp(-2n\alpha_1)$.

In the pass bands of a lossless filter, z_c is real, $\gamma_1=j\beta_1$, $|k_n| = |k_0|$, and the spiral degenerates into a circle about the center of the chart, as in the case of a lossless transmission line.

In the rejection band of a lossless filter the opposite extreme is encountered; z_c is imaginary, $\gamma_1=\alpha_1$, and all of the normalized impedance points lie on a radius of the chart and approach the center as n increases.

Note that any input impedance z_n is easily determined on a Smith chart when z_L, z_c and γ_1 are known.

Graphical Calculation of the Characteristic Impedance of a Lossless Filter

Now let z_L be any real impedance, and define

$$Z_c = \frac{z_c}{z_L} = \frac{1}{a + jb}, \tag{3}$$

$$Z_n = R_n + jX_n = \frac{z_c}{z_L} z_n = \frac{r_n + jx_n}{a + jb}, \quad \text{and} \tag{4}$$

$$K_n = \frac{Z_n - 1}{Z_n + 1} \tag{5}$$

for a lossless filter consisting of n sections (as in Fig. 1).

Since z_c is real in the pass band of a lossless filter, $Z_c=1/a$ and hence

$$z_n = aZ_n = aR_n + jaX_n.$$

Thus

$$k_n = \frac{z_n - 1}{z_n + 1} = \frac{aR_n + jaX_n - 1}{aR_n + jaX_n + 1},$$

and in particular, since $Z_0=1$,

$$k_0 = \frac{a - 1}{a + 1}.$$

Also in the pass band of a lossless filter, $|k_n| = |k_0|$, since γ_n is imaginary, and it follows that

$$\frac{(aR_n - 1)^2 + (aX_n)^2}{(aR_n + 1)^2 + (aX_n)^2} = \frac{(a - 1)^2}{(a + 1)^2}.$$

Solving this equation for a gives

$$a = \pm \sqrt{\frac{R_n - 1}{R_n^2 + X_n^2 - R_n}}. \tag{6}$$

Now in the rejection band of a lossless filter $Z_c=-j/b$, since z_c is imaginary, which implies that

$$z_n = jbZ_n = jbR_n - bX_n$$

and hence that

$$k_n = \frac{z_n - 1}{z_n + 1} = \frac{jbR_n - bX_n - 1}{jbR_n - bX_n + 1} = \frac{(b^2R_n^2 + b^2X_n^2 - 1) + j(2bR_n)}{b^2R_n^2 + (bX_n - 1)^2}. \tag{7}$$

Thus

$$\text{Arg } k_n = \tan^{-1} \frac{2bR_n}{b^2R_n^2 + b^2X_n^2 - 1},$$

and, since $Z_0=1$,

$$\text{Arg } k_0 = \tan^{-1} \frac{2b}{b^2 - 1} = 2\beta_0.$$

Also, since γ_n is real in the rejection band, Arg k_n = Arg $k_0=2\beta_0$. Thus, equating the arguments of k_n and k_0 and solving for b gives

$$b = \pm \sqrt{\frac{1 - R_n}{R_n^2 + X_n^2 - R_n}}. \tag{8}$$

It follows from (3), (6), and (8) that

$$Z_c = \sqrt{\frac{R_n^2 + X_n^2 - R_n}{R_n - 1}}. \tag{9}$$

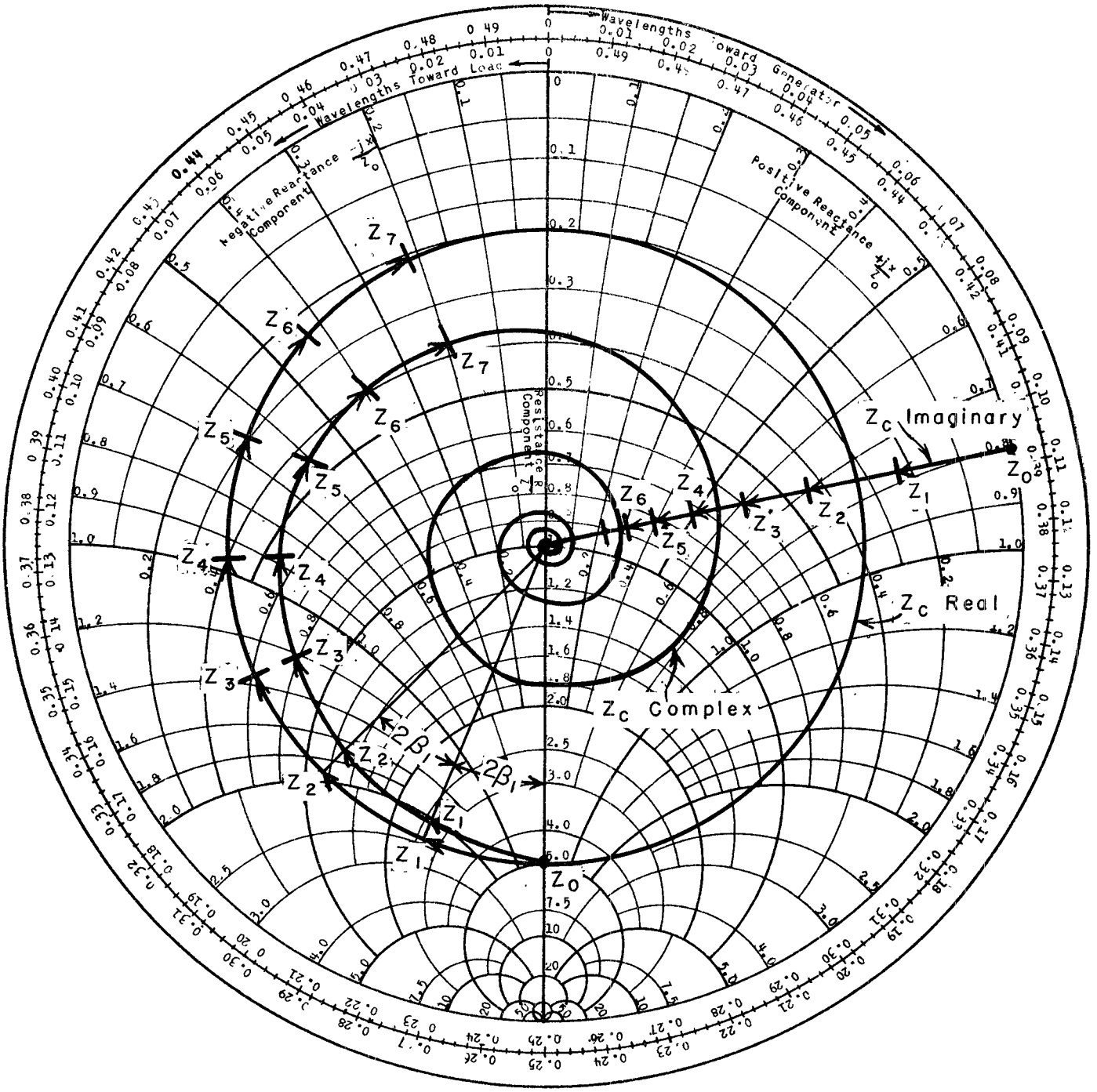

Fig. 2—Typical input impedance plots as a function of the number of filter sections.

From this expression it can be seen that Z_c may be real (in the pass band), imaginary (in the rejection band), or may be either zero or infinite (cutoff conditions) between the rejection and pass bands. The impedance relations $R_n^2+X_n^2=R_n$ and $R_n=1$, corresponding respectively to the two cutoff conditions, are equations of easily identified circles on the Smith chart (see Fig. 3 on the following page), which we shall call *cutoff circles*.

Further consideration of (9) shows that Z_c is real when Z_n lies inside one of the cutoff circles, and is imaginary for all Z_n outside of the cutoff circles. Thus the rejection and pass bands of the filter are easily identified as the sections of the input impedance curve (when normalized to the real load impedance) lying respectively outside or inside of the cutoff circles. The impedance at the cutoff frequency must lie on one of the cutoff circles.

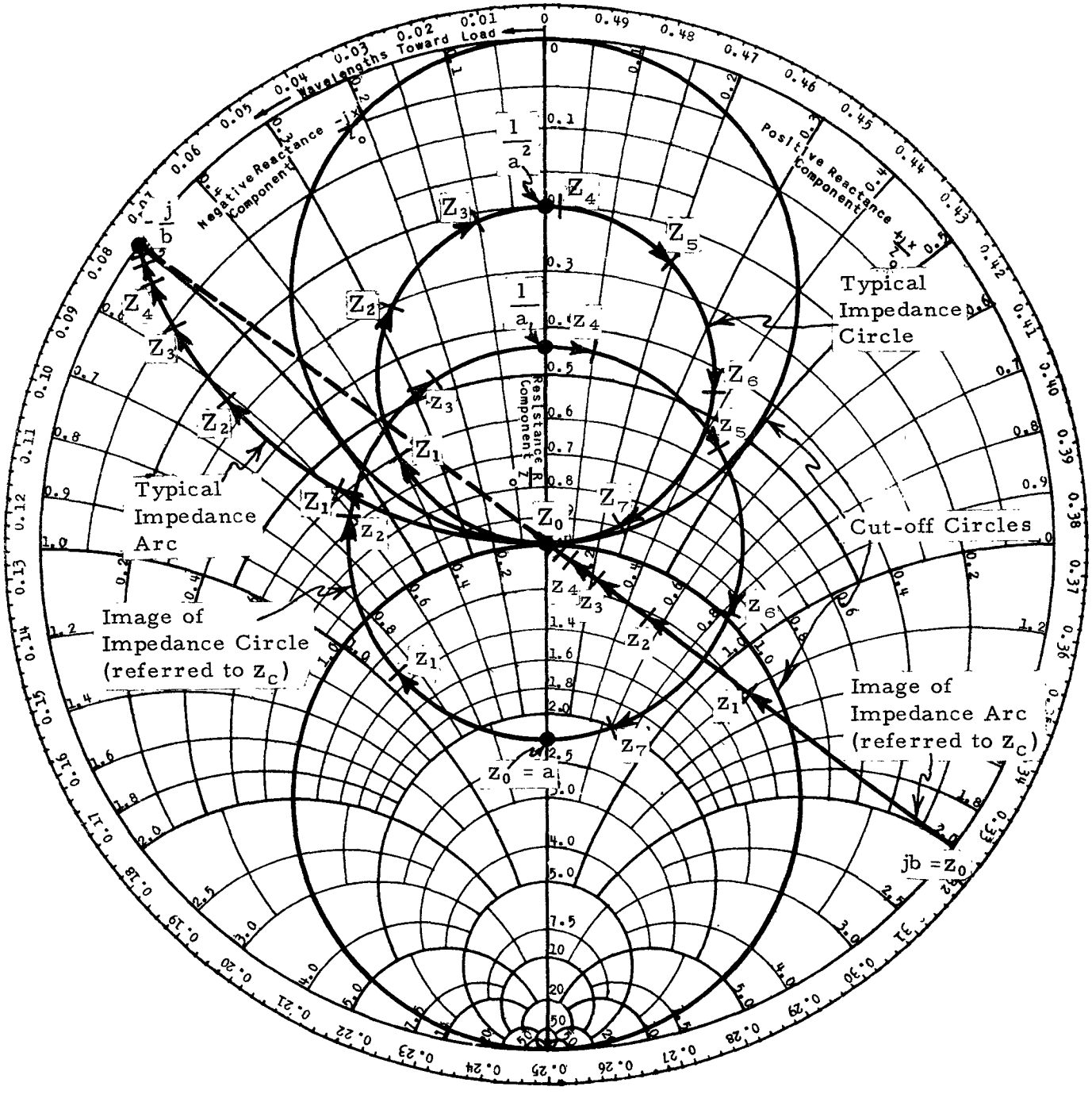

Fig. 3—Cutoff circles and transformations of typical input impedance loci of a lossless filter.

As previously pointed out, the impedances z_n, $n=0, 1, 2, \cdots$, in the pass band lie on a circle about the center of the Smith chart (Figs. 2 and 3). This circle cuts the real axis at the points a and $1/a$.

Since impedance transformations on the Smith chart are bilinear, the impedances Z_n, $n=0, 1, 2, \cdots$, must also lie on a circle, which we shall call an *impedance circle*. This circle cuts the real axis at the origin and at $1/a^2$, as shown in Fig. 3. Thus, when the input impedance Z_n of a filter is known at any frequency in the pass band, the corresponding characteristic impedance can be quickly determined by constructing the unique impedance circle through the known impedance point.

Since the rejection band impedances z_n, which lie along a radius of the Smith chart and approach the center as n becomes large (Figs. 2 and 3), are normalized to the imaginary characteristic impedance, $z_0=jb$ will lie on the rim of the chart.

The impedances Z_n, $n=0, 1, 2, \cdots$, normalized to the real load impedance, z_L, all lie on an arc, which we

shall call an *impedance arc*, and whose center lies on the real axis. (See Fig. 3.) They originate with $Z_0=1$ at the center of the chart and proceed outward along the arc as n increases, approaching the point $Z_c=-j/b$ at which the arc intersects the rim of the chart. Thus when an input impedance is known at a given frequency in a rejection band, the characteristic impedance at that frequency may be quickly determined by constructing the corresponding impedance arc on the Smith chart.

Note that the point $z_0=jb$ is diametrically opposite $Z_c=-j/b$ (see Fig. 3), and that the cutoff circles, the impedance circles, and the impedance arcs all belong to the same family of circles in that they all have a common tangent at the center of the Smith chart.

Calculation of the Attenuation of a Lossless Filter

Consider a lossless filter inserted in an infinite transmission line of characteristic impedance z_L as shown in Fig. 4.

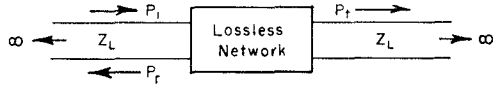

Fig. 4—A lossless network inserted in an infinite transmission line.

Since the filter itself is lossless, the transmitted power

$$P_t = P_i - P_r,$$

where P_i and P_r are the incident and reflected powers respectively, at the input terminals of the filter. Thus the attenuation of the filter with respect to the impedance z_L is

$$\text{Attenuation} = 10 \log \frac{P_i}{P_t} = 10 \log \frac{1}{1-\frac{P_r}{P_i}}$$

$$= 10 \log \frac{1}{1-|K_n|^2}. \qquad (10)$$

Hence the attenuation of a lossless filter may be determined from the Smith chart plot of Z_n. The relation between $|K_n|$ and attenuation is plotted in Fig. 5. A cursor may be calibrated to read attenuation directly from the Smith chart.

Since all Z_n at any given frequency in the pass band lie on the same impedance circle, the maximum reflection coefficient magnitude, and hence the maximum insertion loss, [by (10)], will occur at the point $1/a^2$. This insertion loss cannot be exceeded at the given frequency, regardless of the number of sections in the filter. Thus the impedance circles also give insertion loss information in the pass band.

The attenuation due to the nth section of a lossless filter at any given frequency in the rejection band will, by (10), be

$$A_n = 10 \log \left(\frac{1-|K_{n-1}|^2}{1-|K_n|^2} \right),$$

which may be expressed as

$$A_n = 10 \log \left(\frac{4R_{n-1}}{4R_n} \frac{(R_n+1)^2+X_n^2}{(R_{n-1}+1)^2+X_{n-1}^2} \right),$$

since

$$K_n = \frac{Z_n-1}{Z_n+1} = \frac{R_n+jX_n-1}{R_n+jX_n+1}.$$

It may be seen that

$$A_n \to 10 \log \frac{R_{n-1}}{R_n} \quad \text{as} \quad n \to \infty, \qquad (11)$$

since

$$Z_n \to Z_c = -j/b \text{ as } n \to \infty.$$

It follows from $|k_0|=1$, (since $z_0=jb$), and Arg k_{n-1} = Arg k_n, that

$$\exp(2\alpha_1) = \frac{1}{|k_1|} = \frac{|k_{n-1}|}{|k_n|} = \frac{\text{Im}(k_{n-1})}{\text{Im}(k_n)}.$$

When expressions for Im (k_n) and Im (k_{n-1}) are substituted into this equation from (7), it may be seen that

$$\frac{R_{n-1}}{R_n} \to \frac{1}{|k_1|} \quad \text{as} \quad n \to \infty, \qquad (12)$$

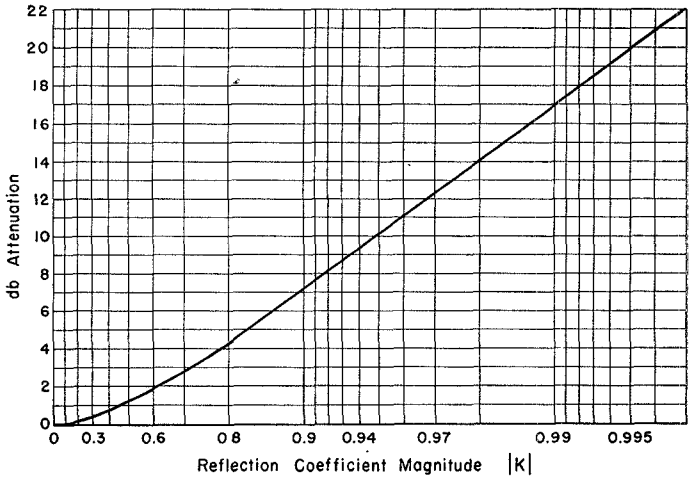

Fig. 5—Attenuation of a lossless network as a function of reflection coefficient.

since z_n approaches the center of the chart. This, together with (11) implies that

$$A_n \to 10 \log \frac{1}{|k_1|} \quad \text{as} \quad n \to \infty,$$

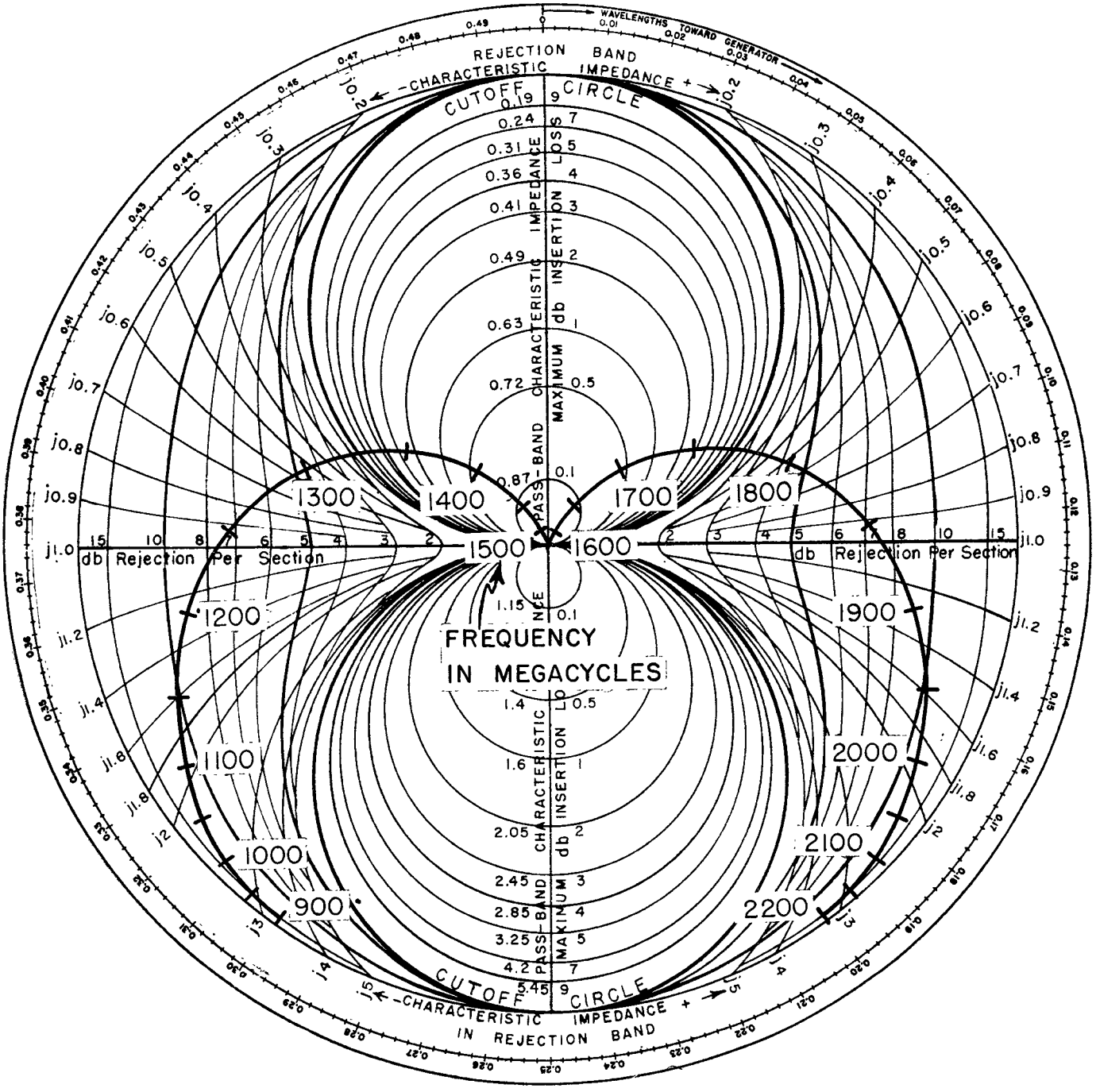

Fig. 6—Typical input impedance curve of a single filter section plotted on a special filter analysis chart.

which will be referred to as the *rejection per section* of the filter at the given frequency.

Thus, for a lossless filter consisting of a number of sections, the rejection at any frequency in the rejection band is approximately

$$n\left(10 \log \frac{1}{|k_1|}\right) = 10 \log \frac{1}{|k_n|} \cdot$$

This approximation is excellent for a large number of sections or when the rejection per section is large.

Filter Analysis Chart

The methods described above can be used to analyze a lossless filter consisting of a number of symmetrical and identical sections from a Smith chart plot of the input impedance when normalized to the real terminating impedance. A similar analysis of a single section will yield the information necessary to predict the characteristics of a filter consisting of any number of such sections. These analyses may be expedited by the use of a chart such as is shown in Fig. 6 in which typical im-

pedance circles and arcs, curves of constant rejection per section, and the cut off circles are constructed as coordinates superimposed on a Smith chart. When a plot of the input impedances of a single section is normalized to its real terminating impedance and plotted on such a chart, the characteristic impedance, the cut off frequencies, and the rejection and pass bands of a filter consisting of any number of these sections can be read directly from the chart and the attenuation properties readily determined. A complete filter may be analyzed in a similar manner.

Note that only one impedance measurement or calculation is required to analyze a filter by this method, instead of the two required for the open and short circuit method, and that when the normalized impedances have been plotted on the filter analysis chart no further calculations are required, since all the information is read directly from the chart.

Note also that, since the terminating impedance z_L can have any real value, it may conveniently be equal to the characteristic impedance of the slotted line used to make the measurements. If the analysis is to be made from calculated impedances, other choices of z_L may be convenient.

Fig. 7 shows the attenuation characteristics of a filter consisting of five of the sections shown, as calculated using the filter analysis chart and as measured on an actual filter. The normalized input impedance is shown plotted on the chart in Fig. 6.

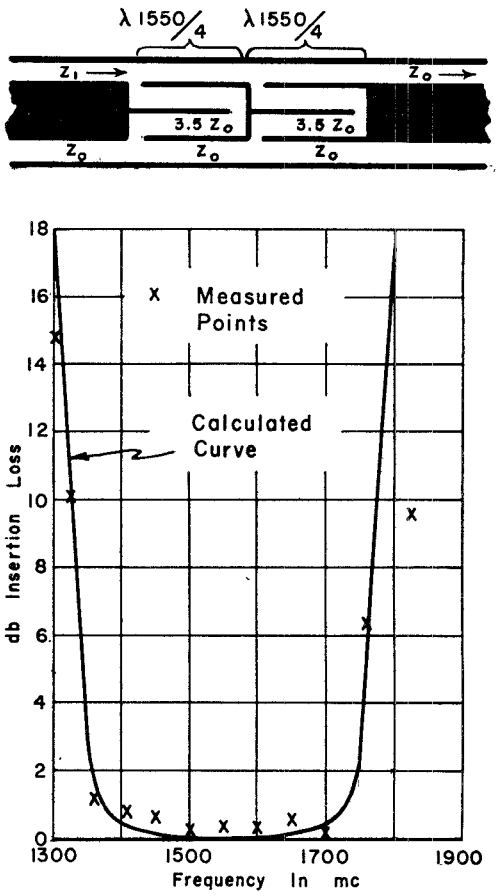

Fig. 7—Calculated and measured characteristics of a filter consisting of five of the sections shown.

Correction

P. D. Strum, author of "Crystal Checker for Balanced Mixers," which appeared on pages 10–15 of the July, 1954 issue of the Transactions, PGMTT, has brought the following correction to the attention of the editors:

In the last paragraph under *Matching Procedure*, " . . . 62-25 . . . " should read " . . . 65-25 . . . ."